Wind Energy Risk Modelling

Wolfgang Karl Härdle*
Brenda López Cabrera*
Awdesch Melzer*°

*Ladislaus von Bortkiewicz Chair of Statistics
*C.A.S.E. – Center for Applied Statistics and Economics
°Institute of Finance
Humboldt-Universität zu Berlin

Hedging on wind

Motivation

- Energy generation soon dominated by renewables
- Wind power highly depends on wind conditions
- Unsteady wind direction may result in zero wind power generation

- Knowledge about variability of wind is essential for
  - Sustainable energy supply and management
  - Secure revenue stream for wind farm operators

Weather futures

- In agriculture: hedging against
  - Rain, drought, snowfall
- In renewable markets: hedging against
  - Unexpected wind conditions, sun duration, clouds

- Market is growing:
  - Nasdaq introduces Wind Power Futures in 2015
  - EEX announces on-site WPF in 2016

Wind power futures

- Contract: A contract settling against the expected on-site power production of future delivery periods

- Underlying: Average wind load factor per contract period

$$CAWP(\tau_1, \tau_2; \phi, \lambda) = \int_{\tau_1}^{\tau_2} P_{\phi,\lambda}(s)ds,$$

where $P_{\phi,\lambda}$ is the average daily load at latitude ϕ and longitude λ, and $\tau_1, \tau_2 (> \tau_1)$ are moments in time.
Alternatives: wind direction, wind speed, wind duration indices.

  - Cumulative Average daily Wind Speed index as basis

$$CAWS(\tau_1, \tau_2; \phi, \lambda) = \int_{\tau_1}^{\tau_2} W_{\phi,\lambda}(s)ds$$

Construction of a wind index

- Wind speed data scattered over a region
- Wind speed at turbine height (extrapolation methods)

- MERRA hourly reanalysis data for Germany
  - Latitude: ϕ : 61 levels at $0.125^\circ \approx$ 10km resolution
  - Longitude: λ : 75 levels at $0.125^\circ \approx$ 10km resolution
  - Time: 8760 hours p.a.
  - Period: 1990-2014: 25 years

Volatility

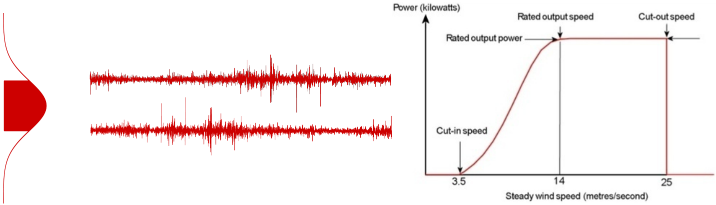

Figure 1: Typically: $\mu_t \pm \sigma_t$
Non-Gaussian world: look at tail event variability related to cut-in and shut down speed. Source: windrocks

Climate volatility

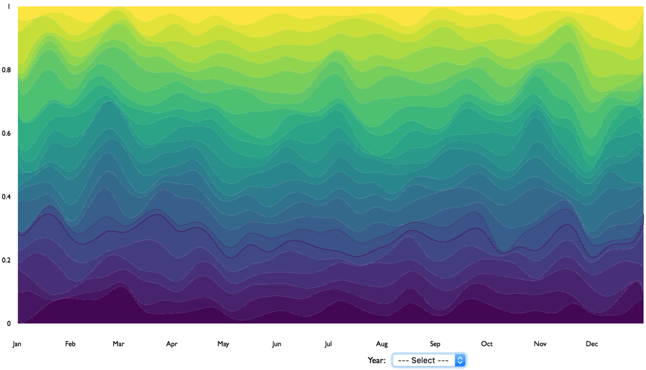

Figure 2: Yearly seasonal inter expectile factor range, estimated for $\phi \cdot \lambda = 61 \cdot 75 = m = 4575$ grid points over Germany, on hourly basis from 1990 to 2014.

Dynamics of volatility: FASTEC

Factorisable Sparse Tail Event Curves for wind speed volatility:

- Common structure of stochastic vola
  - Ultra high dimensional (UHD) time series with factors
  - Sparse penalization with nuclear norm
- Individual variety
  - Tail behaviour
  - Spread analysis on factor loadings
  - Inter Expectile Range as measure of seasonal tail variance

Chao et al. (2015), Huang et al. (2016)

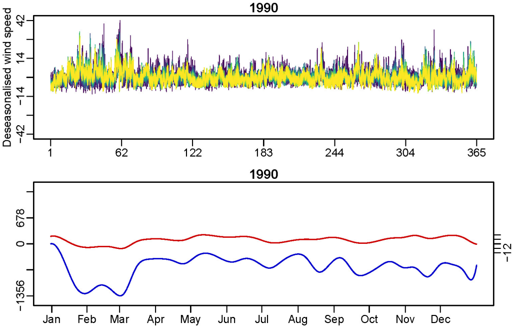

Figure 3: Deseasonalised wind speed and first factor $f_1^{\tau}(\mathbf{X_i}) = \varphi_{\mathbf{1}}^{\top}(\tau)\mathbf{X_i}$, 25% and 99% τ-level. WERMtest

Agenda

1. Motivation ✓
2. Wind index
3. FASTEC methodology
4. Application on wind speed index and forecast.
5. Application to finance: wind energy futures
6. Outlook

Wind speed index

MERRA hourly reanalysis data for Germany at 2m, 10m, 50m

- Latitude: ϕ : 61 levels at $0.125^\circ \approx$ 10km resolution
- Longitude: λ : 75 levels at $0.125^\circ \approx$ 10km resolution
- Frequency: 8760 hours p.a.
- Period: 1990-2014: 25 years

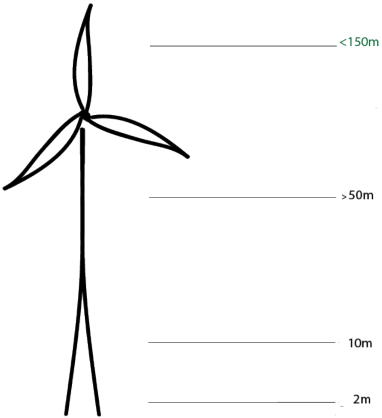

Wind speed at turbine height

- Extrapolate wind speed to higher levels
  - Extended power law (Sen et al. (2012)) ▸ Extended power law
  - Robust shear exponent (Istchenko and Turner (2008)) ▸ Robust shear exponent ▸ $\widehat{\alpha}_t$

	EPL	MERRA50
RMSE	2.992	3.407
MAPE	0.449	0.570

Table 1: RMSE and MAPE for EPL on MERRA10 data and for MERRA50 data from a control area

▸ RSME ▸ MAPE

- For the Wind Power Index
  - Estimate air density (Jones (1978)) ▸ Air density
  - Theoretical wind power ▸ WPD

Measures of tails events

- Loss function, Breckling and Chambers (1988)

  $\rho_{\tau,\gamma}(u) = |\tau - \boldsymbol{I}\{u < 0\}|\,|u|^{\gamma}, \quad \gamma \geq 1$

  $z_{\tau} = \arg\min_{\theta} \mathsf{E}\,\rho_{\tau,\gamma}(Y - \theta)$

  - Quantile - ALD location estimate
    $q_{\tau} = \arg\min_{\theta} \mathsf{E}\,\rho_{\tau,1}(Y - \theta)$

  - Expectile - AND location estimate
    $e_{\tau} = \arg\min_{\theta} \mathsf{E}\,\rho_{\tau,2}(Y - \theta)$

Loss Function

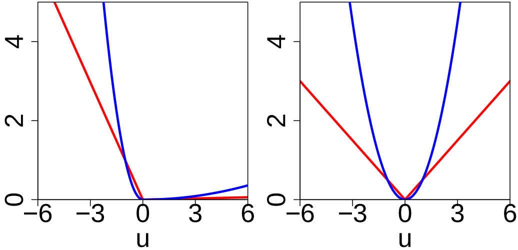

Figure 4: Expectile and quantile loss functions at $\alpha = 0.01$ (left) and $\alpha = 0.50$ (right)

LQRcheck

FASTEC construction

- Data: $\{(\mathbf{X}_i, \mathbf{Y}_i)\}_{i=1}^n$ in $\mathbb{R}^{p+m}$ i.i.d.
- Linear model for τ-expectile curve of Y_j, $j = 1, ..., m, 0 < \tau < 1$:

$$e_j(\tau|\mathbf{X}_i) = \mathbf{X}_i^\top \Gamma_{*j}(\tau), \tag{1}$$

where coefficients for j response: $\Gamma_{*j}(\tau) \in \mathbb{R}^p$

- Sparse factorisation: $f_k^\tau(\mathbf{X_i}) = \varphi_\mathbf{k}^\top(\tau)\mathbf{X_i}$ factors

$$e_j(\tau|\mathbf{X}_i) = \sum_{k=1}^{r} \psi_{j,k}(\tau) f_k^\tau(\mathbf{X}_i), \tag{2}$$

where r : number of factors;
$\Gamma_{*j}(\tau) = (\sum_{k=1}^r \psi_{j,k}(\tau)\varphi_{k,1}(\tau), ..., \sum_{k=1}^r \psi_{j,k}(\tau)\varphi_{k,p}(\tau))$

FASTEC_with_Expectiles

MER formulation: penalised loss

$$\widehat{\Gamma}_\lambda(\tau) = \arg\min_{\Gamma \in \mathbb{R}^{p\times m}} \left\{ (mn)^{-1} \sum_{i=1}^{n} \sum_{j=1}^{m} \rho_\tau \left(Y_{ij} - \mathbf{X}_i^\top \Gamma_{*j} \right) + \lambda \|\Gamma\|_* \right\},$$

$\|\Gamma\|_* = \sum_{j=1}^{\min(p,m)} \sigma_j(\Gamma)$ nuclear norm of Γ

$\mathbf{X}_i$: B-splines

$\mathbf{Y}_i$: wind power density; $(n \times m)$-matrix

Γ : factor matrix

λ : penalisation parameter ▸ Optimal λ

▸ FISTA algorithm

FASTEC: in ultra high dimensional space?

- At each iteration SVD estimation
- Singular Value Decomposition, Principal Component Analysis:
  - $n \to \infty, m = const.$
  - $m \to \infty, n = const.$

  not consistent

Solution: matrix approximation with low-rank features

Cost: increased bias

FASTEC in UHD

- Alternating Least Squares SVD
  - fit a low-rank SVD to a matrix by alternating orthogonal ridge regression ▸ ALS

  Hastie et al. (2014)

- Sparse SVD
  - fast iterative thresholding for low-rank SVD ▸ sSVD

  Yang et al. (2011)

Factor Curves

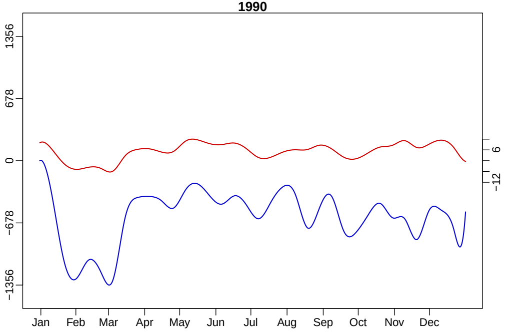

Figure 5: First factor $f_1^\tau(\mathbf{X_i}) = \varphi_1^\top(\tau)\mathbf{X_i}$, at cut-in and shut-down wind speed 25% and 99% τ-level. WERMtest

Wind speed and 1st factor

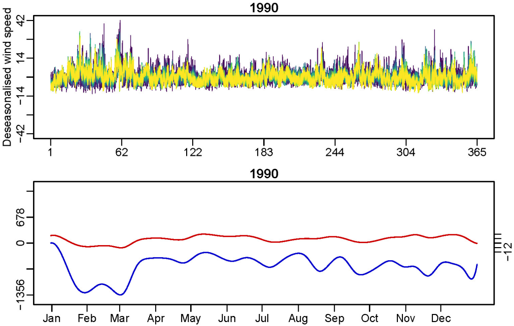

Figure 6: Deseasonalised and centered wind speed and first factor $f_1^{\tau}(\mathbf{X_i}) = \varphi_1^{\top}(\tau)\mathbf{X_i}$, 25% and 99% τ-level. WERMtest

Forecast evaluation

	FASTEC	seasonal AR(3)
RMSE	0.115	0.964
MAPE	0.522	2.087

Table 2: Day ahead (24 hours ahead) forecast-error for the FASTEC and seasonal AR(3) method.

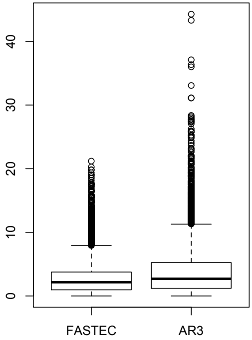

Figure 7: Boxplot of error distributions.

Wind energy futures

- Risk products: wind futures

$$CAWS(\tau_1;\tau_2) = \int_{\tau_1}^{\tau_2} W(s)ds$$

- How to smooth seasonal mean, variance?
- How close are the residuals to $\mathrm{N}(0,1)$?

FEB Four Algorithm

Econometrics

$$
\begin{array}{c}
W_t \\
\downarrow \\
X_t = W_t - \Lambda_t \\
\downarrow \\
X_t = \beta^\top X_{t-L} + \varepsilon_t, \quad \varepsilon_t = \sigma_t e_t \\
\downarrow \\
e_t = \frac{\widehat{X}_t}{\widehat{\sigma}_t} \sim \mathrm{N}(0,1)
\end{array}
$$

Fin. Mathematics

$$
\begin{array}{c}
CAR(3) \\
\downarrow \\
F_{CAWS(t,\tau_1,\tau_2)} \\
\downarrow \\
MPR
\end{array}
$$

Benth et al. (2007), Härdle et al. (2011)

Stylised facts in wind

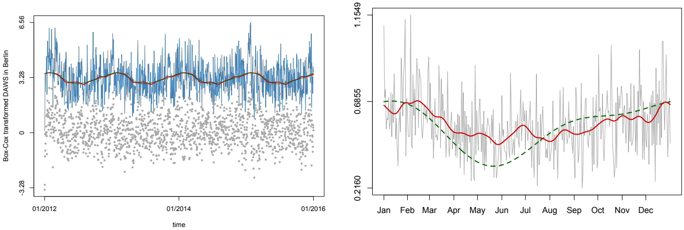

Figure 8: Left: Time series of daily average wind speed in Berlin, with truncated Fourier series (green) and local linear smoothing (red). Right: Seasonal variance. Box-Cox transformation $\widetilde{W_t} = (W_t^\lambda - 1)/\lambda$, with $\widehat{\lambda}_{norm} = 0.375$

Normalisation with the spread of factors

Inter Expectile Range: $|\varphi_{\mathbf{1}}^{\top}(\tau = \mathbf{0.99})\mathbf{X_i} - \varphi_{\mathbf{1}}^{\top}(\tau = \mathbf{0.25})\mathbf{X_i}|$

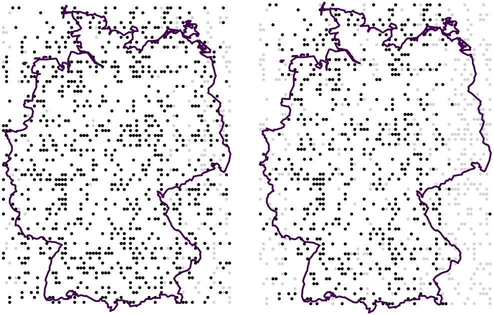

Figure 9: Non-rejection of normality above $\alpha = 0.1$. Left: IER: absolute difference of first factor, explaining around 95% of variability. 73-84% are normal. Right: LL. Estimation for 1000 random points in Germany. 42-57% are normal. Normality tests: Jarque-Bera, Anderson-Darling.

Outlook

- Good performance for modelling risk in weather related energy sources
- Excellent results for normalisation of residuals in the wind derivative pricing algorithm

- Application to Wind Energy Index
- Pricing of Wind Energy Futures

For Further Reading

Benth, F. E., Benth, J. S. and Koekebakker, S. (2007)
Putting a Price on Temperature
Scandinavian Journal of Statistics, **34**, 746-767

Chao, S. K., Härdle, W. and Yuan, M. (2015)
Factorisable Sparse Tail Event Curves
SFB 649 Discussion Paper, **2015-034**

Chao, S. K., Proksch, K., Dette, H.and Härdle, W. (2015)
Confidence Corridors for Multivariate Generalized Quantile Regression
Journal of Business & Economic Statistics, accepted 20150611

Ehm, W., Gneiting, T., Jordan, A., Krüger, F. (2015)
Of Quantiles and Expectiles: Consistent Scoring Functions, Choquet Representations, and Forecast Rankings
eprint: http://arxiv.org/pdf/1503.08195.pdf

George, S.O., George, H.B. and Nguyen, S.V. (2011)
Risk Quantification Associated With Wind Energy Intermittency in California
Power Systems, IEEE Transactions on 26 (4), 1937–1944

Härdle, W. K., Huang, C. and Chao, S.K. (2016)
FASTEC with expectiles
SFB 649 Discussion Paper **2016-008**

Härdle, W. K., Müller, M., Sperlich, S., Werwatz, A. (2004)
Nonparametric and Semiparametric Models
Springer, Berlin

Härdle, W. K., Ló pez Cabrera, B., Okhrin, O. and Wang, W.(2011)
Localising temperature risk
SFB 649 Discussion Paper **2011-001**

Hastie, T., Mazumder, R., Lee, J.D. and Zadeh, R. (2014)
Matrix Completion and Low-Rank SVD via Fast Alternating Least Squares
eprint arXiv:1410.2596

Istchenko, R. and Turner, B. (2008)
Extrapolation of Wind Profiles Using Indirect Measures of Stability
Wind Engineering 32 (5), 433–438

Jones, F.E. (1978)
The Air Density Equation and the Transfer of the Mass Unit
Journal of Research of the National Bureau of Standards, **83** (5), 419–428

Ritter, M., Shen, Z. López Cabrera, B., Odening, M., Deckert, L. (2015a)
A New Approach to Assess Wind Energy Potential
Energy Procedia, 75, 671–676

Ritter, M., Shen, Z. López Cabrera, B., Odening, M., Deckert, L. (2015b)
Designing an index for assessing wind energy potential
Renewable Energy 83, 416–424

Şen, Z., Altunkaynak, A. and Erdik, T. (2012)
Wind Velocity Vertical Extrapolation by Extended Power Law
Advances in Meteorology, doi:10.1155/2012/178623

Ward, K. and Boland,J. (2007)
Modelling the Volatility in Wind Farm Output
eprint:
http://refman.et-model.com/publications/1808/download

Yang, D., Ma, Z., Buja, A. (2011)
A Sparse SVD Method for High-dimensional Data
eprint arXiv:1112.2433v1

Wind Energy Risk Modelling

Wolfgang Karl Härdle[*]
Brenda López Cabrera[*]
Awdesch Melzer[*,°]

[*]Ladislaus von Bortkiewicz Chair of Statistics
[*]C.A.S.E. – Center for Applied Statistics and Economics
[°]Institute of Finance
Humboldt-Universität zu Berlin

WPE: logarithmic law

Logarithmic law

$$\nu_z = \left(\frac{\nu_*}{\kappa}\right) \log \left\{ \frac{(z-d)}{z_0} \right\}$$

ν_z : velocity at height z
ν_* : const. friction velocity
d : displacement height
κ : Kármán const. ≈ 0.41
z_0 : surface roughness Return

WPE: power law

Power law (Istchenko & Turner (2008))

$$\nu_{z_2} = \nu_{z_1} \left(\frac{z_2}{z_1} \right)^{\alpha_t}$$

ν_{z_2} : velocity at height z_2
ν_{z_1} : velocity at reference height z_1, $z_2 > z_1$
α_t : power law coefficient ▸ Return

WPE: extended power law

Extended power law (Sen et al. (2012))

$$\left(\frac{z_2}{z_1}\right)^{\alpha_t} = \left(\frac{\nu_{z_2}}{\nu_{z_1}}\right)$$

rewritten in terms of time averages $\bar{\nu}_{z_i} = T^{-1}\sum_{t=1}^{T}\nu_{z_i,t}$ and perturbation $s_{\nu_{z_i}} = T^{-1}\sum_{t=1}^{T}(\nu_{z_i,t} - \bar{\nu}_{z_i})^2$ at height z_i and 4th order approximation of Binomial expansion.

$$\left(\frac{z_2}{z_1}\right)^{\alpha_t} = \left(\frac{\bar{\nu}_{z_2}}{\bar{\nu}_{z_1}}\right)\left\{1 - \frac{\mathrm{Cov}(\nu_{z_2}\nu_{z_1})}{\bar{\nu}_{z_2}\bar{\nu}_{z_1}} + \frac{s^2_{\nu_{z_1}}}{\bar{\nu}^2_{z_1}} + \frac{s^4_{\nu_{z_1}}}{\bar{\nu}^4_{z_1}}\right\}$$

$$\alpha_t = \frac{\log\left(\frac{\bar{\nu}_{z_2}}{\bar{\nu}_{z_1}}\right) + \log\left\{1 - \frac{\mathrm{Cov}(\nu_{z_2}\nu_{z_1})}{\bar{\nu}_{z_2}\bar{\nu}_{z_1}} + \frac{s^2_{\nu_{z_1}}}{\bar{\nu}^2_{z_1}} + \frac{s^4_{\nu_{z_1}}}{\bar{\nu}^4_{z_1}}\right\}}{\log\left(\frac{z_2}{z_1}\right)}$$

with $t = 1, \ldots, T$, $T = 25$ years $\times$ 365 days $\times$ 24 hours.

Return

Robust shear exponent

Istchenko and Turner (2008) propose

- Median $\widehat{\alpha}_t$ over time of day
- $\widehat{\alpha}_t$ estimated by
  - Power law ▸ Power law
  - Extended power law ▸ Extended power law

▸ Return

Local linear smoothing on $\alpha_{d,h}$

Solving (Härdle et al. (2004))

$$\min_{m,\beta} \sum_{d=1}^{D} \{Y_d - m - (x - x_d)^\top \beta\}^2 K_h(x - x_d),$$

where

$$Y = \begin{pmatrix} Y_1 \\ \vdots \\ Y_D \end{pmatrix}, X = \left\{ \begin{matrix} 1 & (x - x_1)^\top \\ \vdots & \vdots \\ 1 & (x - x_D)^\top \end{matrix} \right\}$$

$$W = \operatorname{diag}\{K_h(x - x_1), \ldots, K_h(x - x_D)\}$$

leads to

$$\widehat{m}_{1,h}(x) = e_0^\top (\mathbf{X}^\top \mathbf{W}\mathbf{X})^{-1} \mathbf{X}^\top \mathbf{W}\mathbf{Y}$$

with $e_0 = (1, 0, \ldots, 0)^\top$.

Optimal bandwidth h for LLS

Estimate h by minimising the cross-validation equation (Härdle et al. (2004))

$$\arg\min_h CV(h;X) = \arg\min_h \sum_{d=1}^{D} \{Y_d - \widehat{m}_{h,-d}(X_d)\}^2 ,$$

where

$$\widehat{m}_{h,-d}(X_d) = \sum_{j \neq d} \frac{K_h(X_d - X_j)Y_j}{\sum_{j \neq d} K_h(X_d - X_j)}$$

Return

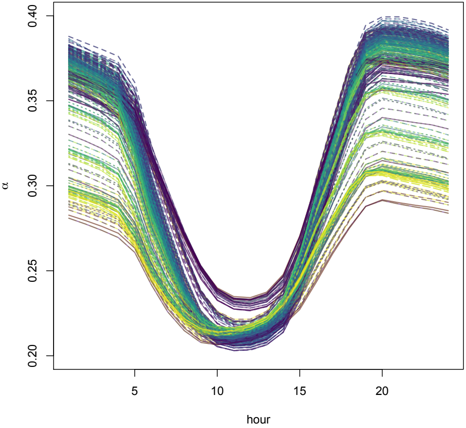

Figure 10: Extended power law: averaged daily $\widehat{\alpha}_t$, based on MERRA velocity data from 01.01.1980-31.12.2014. Return

Air density estimation

Saturation pressure of water vapour E_s based on dewpoint temperature T_d and coefficients c_0, c_1, c_2

$$E_s = c_0 \cdot 10^{c_1 \frac{T_d}{c_2 + T_d}}$$

Use relationship between actual vapour pressure P_v with the saturation pressure E_s at dew point

$$P_v = E_s$$

Dry air pressure P_d, decomposed into total pressure P and pressure due to water vapour P_v

$$P_d = P - P_v$$

Air density estimation

Substitution of above equations leads to air density ρ given temperature T gas constants dry air R_d and water vapour R_v

$$\rho = \frac{P_d}{R_d \cdot T} + \frac{P_v}{R_v \cdot T}$$

Jones (1978)

Return

Potential wind power density

Theoretical wind power density for a fully efficient $\xi = 1$, (standard efficiencies $\xi = 0.2 \sim 0.4$) wind mill

$$WPD_{i,j,t} = \frac{1}{2} \cdot \rho_{i,j,t} \cdot A \cdot \nu^3_{i,j,t}, \quad i \times j : \text{ lat-lon-grid}, t = d \cdot s$$

where A is the area covered by the rotor blades, ρ is air density, ν is velocity.

Return

Fast Iterative Shrinkage Thresholding Algorithm

- Objective: $\min_\Gamma \left\{ F(\Gamma) \overset{def}{=} g(\Gamma) + h(\Gamma) \right\}$
- g: smooth convex function with Lipschitz continuous gradient

$$\| \bigtriangledown g(\Gamma_1) - \bigtriangledown g(\Gamma_2)\|_F \leq L_{\bigtriangledown g} \|\Gamma_1 - \Gamma_2\|_F, \quad \forall \Gamma_1, \Gamma_2$$

  where $L_{\bigtriangledown g} = 2(mn)^{-1} \max(\tau, 1-\tau) \|X\|_F^2$ is the Lipschitz constant of $\bigtriangledown g$
- h: continuous convex function, possibly nonsmooth
- $|F(\Gamma_t) - F(\Gamma^*)| \leq \frac{2L_{\bigtriangledown g} \|\Gamma_0 - \Gamma^*\|_F^2}{(t+1)^2}$

FISTA algorithm

1. Initialise: $\Gamma_0 = 0, \Omega_1 = 0$, step size $\delta_1 = 1$
2. For $t = 1, 2, \dots, T$
   - $\Gamma_t = \arg\min_\Gamma \left[\frac{g(\Gamma)}{L_{\bigtriangledown g}} + \frac{1}{2} \left\| \Gamma - \left\{ \Omega_t - \frac{1}{L_{\bigtriangledown g}} \bigtriangledown g(\Omega_t) \right\} \right\|^2 \right]$
   - when penalising nuclear norm $\Gamma_t = \mathbf{P} \left(\mathbf{R} - \frac{\lambda}{L_{\bigtriangledown g}} \mathbf{I}_{p \times m} \right) \mathbf{Q}^\top$, and $\Omega_t - \frac{1}{L_{\bigtriangledown g}} \bigtriangledown g(\Omega_t) = \mathbf{PRQ}^\top$ with ALS-SVD (Hastie et al. (2014)) or sparse SVD (Yang et al. (2011))
   - $\delta_{t+1} = \frac{1 + \sqrt{1 + 4\delta_t^2}}{2}$
   - $\Omega_{t+1} = Gamma_t + \frac{delta_{t-1}}{t+1} (\Gamma_t - \Gamma_{t-1})$
3. $\widehat{\Gamma} = \Gamma_T$

Return

ALS-SVD algorithm

1. Initialise $A = UD$, $U_{m\times r}$ is randomly chosen matrix with orthonormal columns and $D = I_r$
2. Given A, solve for B
   - $\min_B \|X - AB^\top\|_F^\top + \lambda\|B\|_F^2$
   - $\widetilde{B}^\top = (D^2 + \lambda I)^{-1} DU^\top X$
3. Compute SVD $\widetilde{B}D = \widetilde{V}\widetilde{D}^2\widetilde{R}^\top$, let $V \leftarrow \widetilde{V}, D \leftarrow \widetilde{D}, B = VD$
4. Given B, solve for A
   - $\min_A \|X - AB^\top\|_F^\top + \lambda\|A\|_F^2$
   - $\widetilde{A}^\top = XVD(D^2 + \lambda I)^{-1}$
5. Compute SVD $\widetilde{A}D = \widetilde{U}\widetilde{D}^2\widetilde{R}^\top$, let $U \leftarrow \widetilde{U}, D \leftarrow \widetilde{D}, A = UD$
6. Repeat (2)-(5) until convergence of $AB^\top$
7. Compute $M = XV$, its SVD $M = UD_\sigma R^\top$, output: $U, V \leftarrow VR, \mathcal{S}_\lambda(D_\sigma) = diag\{(\sigma_1 - \lambda)+, \ldots, (\sigma_r - \lambda)\}$

▸ Return

FIT-SSVD algorithm

input Observed X, target rank r, threshold function η ▸ η, initial orthonormal matrix $V^{(0)} \in \mathbb{R}^{p \times r}$, threshold level γ ▸ γ,

output $\widehat{U}, \widehat{V}$

repeat

- R-2-L-×: $U^{(k),\times} = XV^{(k-1)}$
- L-thresholding: $U^{(k),thr} = \eta\left(U_{il}^{(k),\times}, \gamma_{ul}\right)$, where
  $\gamma_{ul} = f(X, U^{(k-1)}, V^{(k-1)}, \widehat{\sigma}), \widehat{\sigma} = 1.4826 \cdot MAD(X)$
- L-orthonormalisation QR-decomposition: $U^{(k)} R_u^{(k)} = U^{(k),thr}$
- L-2-R-×: $V^{(k),\times} = X^\top U^{(k)}$
- R-thresholding: $V^{(k),thr} = \eta\left(v_{jl}^{(k),\times}, \gamma_{vl}\right)$, where
  $\gamma_v = f(X^\top, V^{(k-1)}, U^{(k)}, \widehat{\sigma})$
- R-orthonormalisation QR-decomposition: $V^{(k)} R_v^{(k)} = V^{(k),thr}$

until convergence

▸ Return

Thresholding function η

- Allow any thresholding function $\eta(x,\gamma)$, satisfying $|\eta(x,\gamma) - x| \leq \gamma$ and $\eta(x,\gamma)\mathbf{1}_{|x|\leq\gamma}$
  - Soft-thresholding: $\eta_{soft}(x,\gamma) = sign(x)(|x| - \gamma)_+$
  - Hard-thresholding: $\eta_{hard}(x,\gamma) = x\mathbf{1}_{|x|>\gamma}$
  - SCAD-thresholding: $\mathrm{sign}(x)\mathbf{1}_{|x|\geq\gamma}\mathbf{1}_{|x|\leq 2\gamma}\frac{((\alpha-1)x-\mathrm{sign}(x)\alpha\gamma)}{(\alpha-2)}\mathbf{1}_{2\gamma<|x|}\mathbf{1}_{|x|\geq\alpha\gamma}+x\mathbf{1}_{|x|>\alpha\gamma}$

Return

Data: $X \in \mathbb{R}^{n\times p}$, $U^{(k)} \in \mathbb{R}^{n\times r}$, $V^{(k)} \in \mathbb{R}^{p\times r}$, number of bootstraps M, standard deviation of noise $\widehat{\sigma}$

Result: Threshold level $\gamma \in \mathbb{R}^r$

Subset: $L_u = \{i : u^{(k)}_{i1} = \ldots = u^{(k)}_{ir} = 0\}, H_u = L_u^c, H_v = L_v^c$;

$L_v = \{j : v^{(k)}_{j1} = \ldots = v^{(k)}_{jr} = 0\}$;

if $|L_v||L_u| < n|H_v|\log(n|H_v|)$ **then**

  return $\gamma = \widehat{\sigma}\sqrt{2\log(n)}\mathbf{1} \in \mathbb{R}^r$;

else

  for $i \leftarrow 1$ **to** M **do**

    Sample $n|H_v|$ entries from $X_{L_u L_v}$ and reshape them into a matrix $\widetilde{Z} \in \mathbb{R}^{n\times|H_v|}$;

    $B = \widetilde{Z}V^{(k)}_{H_v:} \in \mathbb{R}^{n\times r}$; $C_{i:} = (\|B_{:1}\|_\infty, \|B_{:2}\|_\infty, \|B_{:r}\|_\infty)^\top$;

  end

  $\gamma_l =$ median$(C_{:l})$; **return** $\gamma = (\gamma_1, \ldots, \gamma_r)^\top$.

end

▸ Return

Some assumptions

- $\{(\mathbf{X}_i, \mathbf{Y}_i)\}_{i=1}^{n} \in \mathbb{R}^{p+m}$ are i.i.d., $\{X_i\}_{i=1}^{n} \in \mathbb{R}^{p} \sim \mathsf{N}(0, \Sigma)$
- Conditional on $\mathbf{X}_i$, $u_{ij} = \{Y_{ij} - \mathbf{X}_i^\top \Gamma_{\cdot j}\}_{j=1}^{m}$ are cross-sectional independent over j
- $u_{i1}, \dots, u_{im}$ are sub-gaussian: $\exists C > 0$ s.t. $\mathsf{P}(|u_{ij}| > s) \leq \exp\{1 - \left(\frac{s}{C}\right)^2\}, j \in \{1, \dots, m\}$
- $K_u \overset{def}{=} \max_{1 \leq j \leq m} \|U_{ij}\|_{\psi_2} = \max_{1 \leq j \leq m} \sup_{p \leq 1} p^{-\frac{1}{2}} (\mathsf{E}\,|u_{ij}|^p)^{\frac{1}{p}}$

Optimal choice of tuning parameter λ

- Under the assumptions of sample setting, selecting

$$\lambda = \frac{2}{m} S \max(\tau, 1-\tau) \sqrt{K_u^2 \|\Sigma\| \frac{p+m}{n}}, \quad \text{for } n \leq 2\min(m,p)$$

any optimal solution $\widehat{\Gamma}_\lambda$ satisfies error bound conditions (Huang et al. (2016))

- Then

$$P\left\{ \| \bigtriangledown g(\Gamma)\| \leq m^{-1} S \max(\tau, 1-\tau) \sqrt{K_u^2 \|\Sigma\| \frac{p+m}{n}} \right\}$$
$$\leq 1 - 3 \cdot 8^{-(p+m)} - 4\exp(-n/2),$$

where S is an absolute constant.

Return

Root mean squared error

$$RMSE = \sqrt{\frac{\sum_{t=1}^{n} (\widehat{y}_t - y_t)^2}{n}}$$

Return

Mean absolute percentage error

$$MAPE = \frac{1}{n}\sum_{t=1}^{n}\left|\frac{y_t - \widehat{y}_t}{y_t}\right|$$

Return